

RESEARCH

Open Access



An Experimental Study of Shear Resistance for Multisize Polypropylene Fiber Concrete Beams

Xin Yang^{1,2,3}, Ninghui Liang^{1,2*}, Yang Hu^{1,2} and Rui Feng⁴

Abstract

To study the influence of polypropylene fibers with different thicknesses on concrete beams, inclined section shear tests of polypropylene fiber concrete beams were carried out. The cracking load, ultimate load, midspan deflection, reinforcement, and strain of polypropylene fiber concrete beams and conventional reinforced-concrete beams under shear were compared and analyzed. The load-bearing capacity of the rectangular beams was improved significantly by polypropylene fiber addition. Compared with conventional reinforced-concrete beams, the limit shear load of concrete beams with polypropylene fibers and multisize polypropylene concrete beams that were reinforced with three types of fibers increased by 8.67% and 17.07%, respectively. By mixing polypropylene fibers into concrete beams, the initial crack shear force of the beam was improved, the number of cracks was increased and the crack width was reduced, which can increase the beam ductility, inhibit crack formation and increase the strength. The computational formula of the shear ultimate bearing capacity of polypropylene fiber–concrete beams was revised according to composite material theory, and the calculated results were consistent with the test values.

Keywords: fiber-reinforced concrete beam, polypropylene fibers, shear resistance, multisize, computational formula

1 Introduction

Polypropylene fibers can be classified as coarse and fine fibers. Fine polypropylene fibers are relatively small, can refine cracks after being mixed with concrete, improve the original defects of the concrete structure to a certain extent and inhibit cracks. The coarse polypropylene fiber diameter varies from 0.1 to 1.0 mm, and its surface is profiled by rolling. Compared with fine polypropylene fibers, coarse polypropylene fibers can bond tighter with concrete and the bearing capacity for each fiber is larger. In recent years, many scholars have researched the action mechanism of fiber concrete beams and many research results have been obtained. Thomas and

Ramaswamy (2006) studied the shear strength of prestressed steel–fiber-reinforced concrete T-beams, it is shown that the shear capacity of partially prestressed concrete beams can be significantly improved by providing fiber reinforcement. Khalid et al. (2018) used recycled plastic waste as a fiber in concrete beams and found that a higher amount of fiber resulted in a higher concrete structure tensile strength. Aoude et al. (2012) conducted tests on reinforced concrete and steel–fiber-reinforced concrete beams and studied the influence of steel fibers on the shear-bearing capacity, failure mechanism and crack control, it is found that the addition of fibers leads to improved shear resistance in shear-deficient beams. Ma et al. (2018) studied the compressive strength, tensile strength and bending strength of concrete with mixed fibers, and found that a 1.5% volume fraction of long steel fibers and a 0.5% volume fraction of short steel fibers can provide the best bending strength. Hu et al. (2004) studied the influence of fiber orientation, beam

*Correspondence: cqulnh@163.com

¹ School of Civil Engineering, Chongqing University, Chongqing 400045, China

Full list of author information is available at the end of the article
Journal information: ISSN 1976-0485 / eISSN 2234-1315

length and reinforcement ratio on the ultimate strength of the beams. The application of fiber-reinforced plastics can improve the stiffness and ultimate strength of the reinforced concrete beams significantly. Khan et al. (2011) established a constitutive model for the elastic failure of concrete members, including concrete fracture, carbon-fiber-reinforced polymer fracture and concrete carbon-fiber-reinforced polymer interface failure. Lee (2017) evaluated the influence of concrete strength and fiber content on the concrete proportional limit, residual bending strength and energy absorption capacity, it is shown that fiber-reinforced concrete beams with a strength of 45 MPa show a high increase in residual flexural strength immediately after concrete cracking, especially for 0.5% fiber volume fraction. Ferreira et al. (2016) found that reinforced concrete with mixed fibers showed an excellent toughness because of the interaction between fibers. Nordin and Taljsten (2004) studied the bending property of concrete beams with mixed fibers. Sahoo et al. (2015) found that the displacement ductility of beam specimens increased by 120% with polypropylene fiber addition with a volume fraction of 1%. In all beam specimens, a better postpeak residual strength response resulted because of multi-place cracks that were caused by fiber bridging. Cardoso et al. (2019) studied the bending characteristics of steel–fiber-reinforced concrete beams, it is found that compared with ordinary reinforced concrete beams, the bearing capacity of steel–fiber-reinforced concrete beams is increased by 21 to 109%, and the crack opening is significantly reduced under a given reinforcement stress. Asgari et al. (2019) found that the glass–fiber-reinforced concrete layer can improve the bearing capacity and ultimate deflection of the beam significantly by strengthening the concrete beam by the section expansion method. Abdelrazik et al. (2020) discussed the influence of fiber type and volume on properties of fiber-reinforced concrete. Younis et al. (2020) reports on the results of an experimental study on the short-term flexural performance of seawater-mixed recycled-aggregate concrete beams, it is found that GFRP-RC beams show higher bearing capacity, but lower deformation characteristics compared with reinforced concrete beams. Liu et al. (2016; Zhang et al., 2018) studied the effects of fiber types and hybrid modes on the tensile behavior, flexural toughness and fracture mechanical properties of ultrahigh-performance concrete, it is shown that the critical value of substitution rate of coarse aggregate is 25%, and the effects of different fiber types on compressive strength are similar. Raja et al. (2020) studied the effect of size and quantity of coarse aggregate on the fracture behavior of steel fiber-reinforced self-compacting concrete, it is argued that the fracture energy increases with the increase of the size and quantity of

coarse aggregate. Meesala (2019) discussed three types of fibers on the properties of recycled-aggregate concrete; it is found that the fiber significantly improves the mechanical properties of conventional and recycled-aggregate concrete. Saje et al. (2011) found that the shrinkage of the fiber-reinforced concrete was considerably reduced by increasing the content of the fibers up to 0.5% of the volume of the composite. Koniki and Prasad (2019) pointed out that short and fine fibers enhance the fresh property of concrete by controlling the growth of micro-cracks, and long and coarse fibers enhance the hardening property of concrete by arresting the propagation of macro-cracks. Melian et al. (2010) discussed the low fractions of polypropylene short fibers to increasing toughness of self-compacting concrete. Hameed et al. (2020) found that the negative effect of recycled aggregates could be minimized by the addition of polypropylene fibers. Das et al. (2018) revealed that the fibers play an important role in determining the split tensile and flexural strength of concrete, whose maximum increments are 12.01% and 17.15% for split and flexural strength values. Xu et al. (2017) (Deng et al., 2018; Huang et al., 2019) studied bond strength of deformed reinforcement embedded in steel polypropylene hybrid fiber-reinforced concrete matrix and the interfacial bonding properties of steel fibers in steel polypropylene hybrid fiber-reinforced cement-based composites, it is found that compared to the specimen made with plain concrete, the introduction of hybrid fibers could exert obvious positive influences on the bond strength. Gail and Subramaniam (2019) investigated the link between the fracture behavior and shear capacity of fiber-reinforced concrete composite. Spinella et al. (2012) predicted the complete load-versus-displacement curves by suitably adapting a nonlinear finite element code for plain and reinforced concrete. Zhang et al. (2014) studied shear behavior of polypropylene fiber-reinforced ECC beams with varying shear reinforcement ratios. Navas et al. (2020) studied on the shear behavior of macrosynthetic fiber-reinforced concrete beams and compared them to steel fiber-reinforced concrete beams. Arslan et al. (2017) found that both the shear strength and ductility of the beams were improved by adding polypropylene fibers, but the addition of polypropylene fibers even at 3% by volume was not able to change the failure mode for beams with shear span-to-effective depth ratios of 2.5 and 3.5.

This paper studies the reinforcement effect of polypropylene fibers on concrete beams. Three groups of beams, B0, B1 and B2, were designed and fabricated, with three beams in each group and nine test beams in total. B0 was a conventional reinforced-concrete beam and will serve as a control group. B1 was a concrete beam that is mixed only with coarse polypropylene fibers. B2 was a multisize

polypropylene fiber concrete beam that was mixed with two fine polypropylene fiber types and one type of coarse polypropylene fiber. It is of great theoretical and practical significance to reveal the action mechanism of coarse and fine polypropylene fibers through inclined section shear tests.

2 Experimental Scheme Design

The geometric dimensions, longitudinal reinforcement ratio, stirrup reinforcement ratio and mix proportions of nine rectangular concrete beams were the same. The cross-sectional dimensions of all rectangular beams were $b \times h \times l = 150 \text{ mm} \times 300 \text{ mm} \times 2150 \text{ mm}$ (see Fig. 1 for the geometric dimensions and reinforcement drawings).

2.1 Experimental Materials and Design of Mix Proportions

The experimental materials were:

- (1) Cement: 42.5R conventional Portland cement produced by Hongshi Cement Co., Ltd.
- (2) Sand: manufactured sand with a fineness modulus of 3.1 and a loose bulk density of 1530 kg/m^3 , extra-

fine sand with a fineness modulus of 0.8 and a loose bulk density of 1294 kg/m^3 .

- (3) Stone: gravel (5 to 10 mm) from Gele Mountain, Chongqing, with a silt content of 0.5%, an apparent density of 2680 kg/m^3 and a loose bulk density of 1385 kg/m^3 ; gravel (10 to 20 mm) from Gele Mountain, Chongqing, with a silt content of 0.7%, an apparent density of 2690 kg/m^3 and a loose bulk density of 1405 kg/m^3 .
- (4) Water reducer: a type of polycarboxylate superplasticizer.
- (5) Polypropylene fiber: fibers (CF1) produced by Ningbo Dacheng Advanced Material Co., Ltd. were used as coarse polypropylene fibers, and fibers (FF1, FF2) that were produced by Hebei Qingjun Cellulose Factory were used as fine fibers. Specific physical performance parameters are shown in Table 1 and Fig. 2.

The mix proportions of concrete were as follows according to reference (JGJ, 2019): cement:water:sand:stone:water reducer = 380:175:701:1144:3.80. C30 concrete was used with a water:cement ratio of 0.46. The fiber content was determined according to the test design and the recommended fiber content of the manufacturer. The recommended fine fiber content was 0.9 kg/m^3 , and the recommended coarse fiber content was 6.0 kg/m^3 . Table 2 shows the mix proportions of the materials. The A0 reference specimen was poured as conventional reinforced concrete. A1 was a test piece that was mixed with coarse polypropylene fiber CF1, and the fiber content was 6.0 kg/m^3 . A2 was a specimen that was mixed with three polypropylene fiber types, and the FF1, FF2 and CF1 contents were 0.6 kg/m^3 , 0.6 kg/m^3 and 4.8 kg/m^3 , respectively.

The performance test results of reinforcement are shown in Table 3.

2.2 Preparation and Curing of Concrete Beams

Pour the weighed sand and stone into the mixer, start the mixer and mix for about 1 min, and then evenly disperse the polypropylene fiber into the mixer with the mixing. After the fiber is sprinkled, continue to stir for about

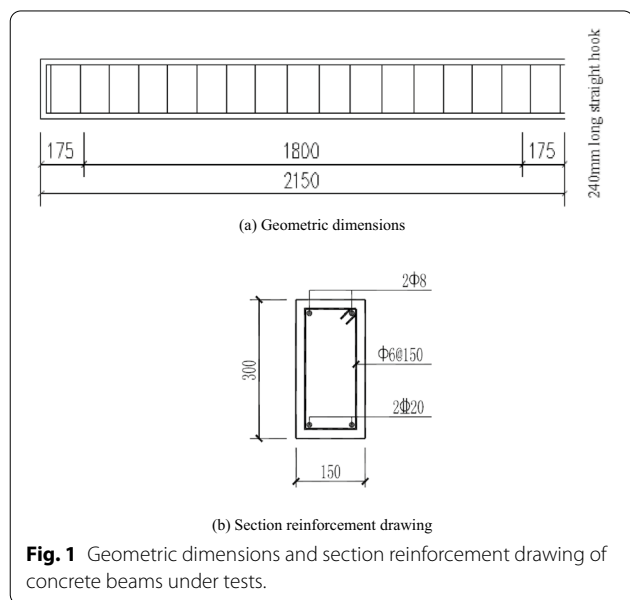


Fig. 1 Geometric dimensions and section reinforcement drawing of concrete beams under tests.

Table 1 Physical and mechanical indices of polypropylene fibers.

Fiber no.	Equivalent diameter (μm)	Length (mm)	Tensile strength (MPa)	Elastic modulus (GPa)	Elongation at break (%)	Density (g cm^{-3})	Recommended dosage (kg m^{-3})
FF1	26.1	19	641	4.5	40	0.91	0.9
FF2	100	19	322	4.9	15	0.91	0.9
CF1	800	50	706	7.4	10	0.95	6.0

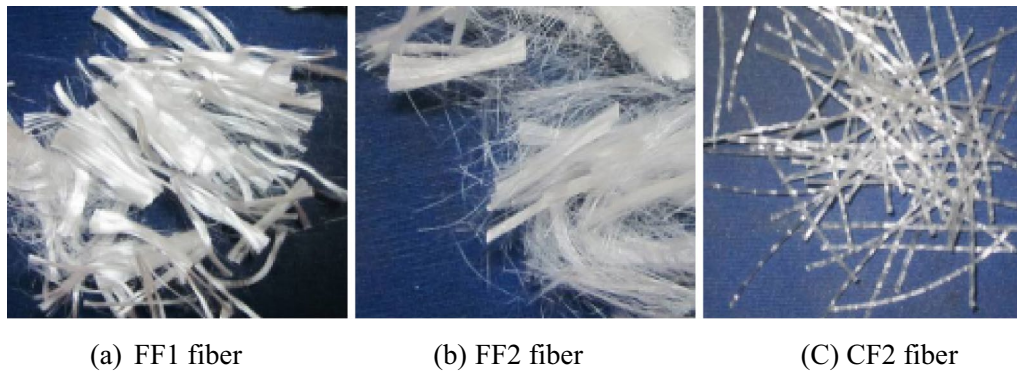


Fig. 2 Polypropylene fibers.

Table 2 Mix proportions of C30 concrete/(kg m⁻³).

Specimen no.	Fiber type	Cement	Sand	Stone	Water	Sand ratio (%)	Fiber content	Water reducer (%)
A0	None	380	701	1144	175	38	0	1
A1	CF1	380	701	1144	175	38	6.0	1
A2	FF1 + FF2 + CF1	380	701	1144	175	38	0.6 + 0.6 + 4.8	1

Table 3 Mechanical properties of reinforcement.

Reinforcement strength grade	Diameter (mm)	Area (mm ²)	Yield strength (MPa)	Yield strain (× 10 ⁻⁶)	Elastic modulus (Gpa)
HPB235	6	28.3	402.00	1927	208.66
HPB235	8	50.3	355.67	1387	256.43
HRB400	16	201.1	433.61	2278	190.31

2 min. During the mixing process, stop the mixer to see if there is fiber agglomeration. If so, take it out and disperse it, and then put it evenly into the mixer to continue mixing. Slowly pour the weighed cement into the mixer and mix for 2 min. Add water reducer into the water in advance and add it to the mixer during mixing. At this time, it can be observed that the fibers in the concrete have been evenly dispersed. Observe the change of concrete properties, if the dry humidity is suitable and there is no coarse aggregate submerge, it proves that the mixing degree meets the needs and has been successful.

If fibers can distribute evenly when they are mixed into concrete, the initial defects of the concrete structure will be improved significantly, and the performance will be better, thus the performance of the concrete is improved. Because of the low elastic modulus of polypropylene fibers, if the fibers cannot be evenly distributed, bunched or clustered in concrete, it may degrade the concrete performance, pose adverse impacts and lead to a failure to

meet engineering needs. Therefore, higher requirements often exist on the dispersibility of the fibers to ensure that they can be distributed evenly during casting and reach all parts of the concrete structure to avoid fiber aggregation. Curing was carried out in a standard curing room for 28 days, at 20 ± 2 °C, with a humidity above 90%; see Fig. 3.

2.3 Data Collection and Arrangement of Measure Point

The measure points of each beam were arranged as follows: (1) a 50-ton load sensor was used to collect the concentrated load on the beam; (2) a dial gage (connected with a strain-testing system after calibration) was used to collect the span deflection in the beam span and at the support; (3) a 80-mm strain gage was used to measure the through the thickness strain of the cross-section concrete 250 mm from the left support. The specific arrangement of each measure point is shown in Fig. 4.

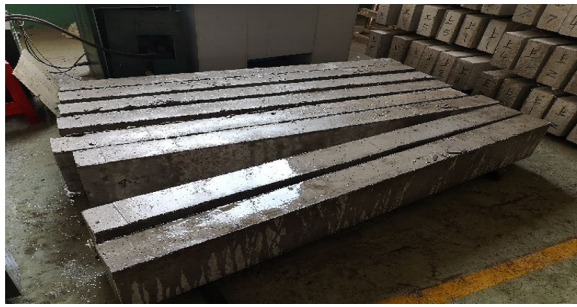


Fig. 3 Cured concrete beams after pouring.

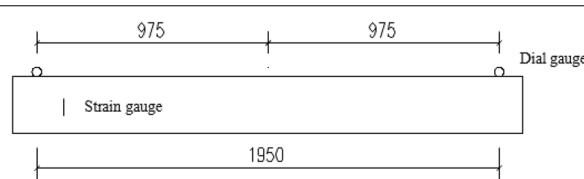


Fig. 4 Arrangement of measure point of test beams.

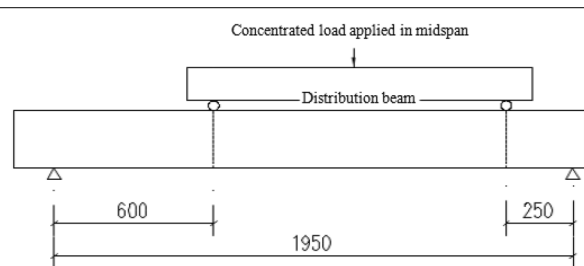


Fig. 5 Loading schematic diagram of beams under test.

2.4 Loading Equipment and Loading Scheme

A 5000-kN electrohydraulic servo pressure testing machine was used to apply force to the distribution beam so that the shear span ratio λ was 2.26 (the shear span ratio was the ratio of section bending moment to the product of shear force and effective height). Pre-loading was carried out in three stages, with each stage taking 5% of the estimated limit load of the test beams. Instruments and equipment were unloaded to 0 MPa after confirming that the beams operated normally, and formal loading commenced. Graded loading was used in the loading process, at 10 kN for each grade. When the predicted cracking load was approached, the load for each grade was halved, to obtain the load value at the first crack is found. A schematic diagram of the test loading is shown in Fig. 5.

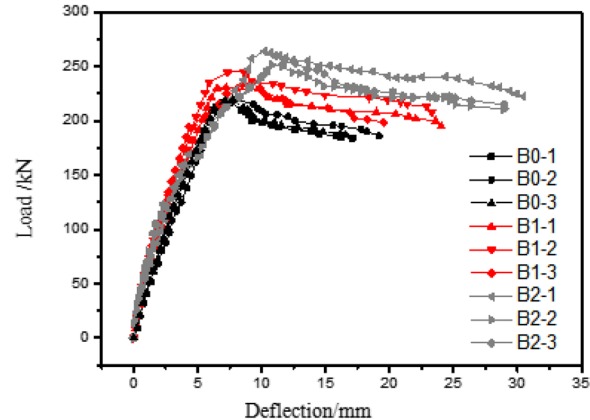


Fig. 6 Load-midspan deflection curve of test beam.

3 Experimental Results and Analysis

3.1 Load-Midspan Deflection Curve

For beams in the shear tests, the shear-load point-displacement curve and the load-midspan deflection curve of the beams can reveal the macro-characteristics of the test beams after loading. The load-midspan deflection curve was used to analyze the shear-bearing capacity of the test beams. The load-midspan deflection curve of the test beams is shown in Fig. 6, and the midspan deflection that corresponds to the ultimate load is shown in Table 4, in which the B0 test team used an A0 specimen, the B1 test team used an A1 specimen and the B2 test team used an A2 specimen as concrete, respectively.

For convenience of analysis, the average load-midspan deflection curve, ultimate beam load and corresponding midspan deflection of each group of test beams B0, B1 and B2 are shown in Table 4 and Fig. 7:

By analyzing Fig. 7, the following results can be obtained:

- (1) Polypropylene fiber addition into concrete can improve the ultimate shear capacity of the inclined section of the concrete beams. Compared with conventional reinforced-concrete beams, the ultimate shear-bearing capacities of concrete beam B1 mixed with coarse polypropylene fibers and B2 mixed with three fiber types increased by 8.67% and 17.07%, respectively.
- (2) A comparison of the midspan deflection that corresponds to the ultimate load of the three beam groups shows that the midspan deflection of B1 and B2 increased by 9.68% and 50.84%, respectively, compared with B0, i.e., polypropylene fiber addition increases the shear beam ductility. Multisize polypropylene fiber addition with three fiber types can improve the beam toughness significantly.

Table 4 Ultimate load of test beam and corresponding midspan deflection.

Test beam no.	Limit load (kN)	Average limit load (kN)	Midspan deflection corresponding to ultimate load (mm)	Average midspan deflection corresponding to ultimate load (mm)	Standard deviation of the average limit loads (kN)
B0 B0-1	217.10	218.79	7.60	7.75	1.23
B0-2	220.00		7.90		
B0-3	219.27		7.76		
B1 B1-1	229.65	236.45	9.80	9.22	6.56
B1-2	245.32		8.61		
B1-3	234.37		9.24		
B2 B2-1	263.94	257.04	10.22	10.92	5.04
B2-2	252.07		10.77		
B2-3	255.10		11.77		

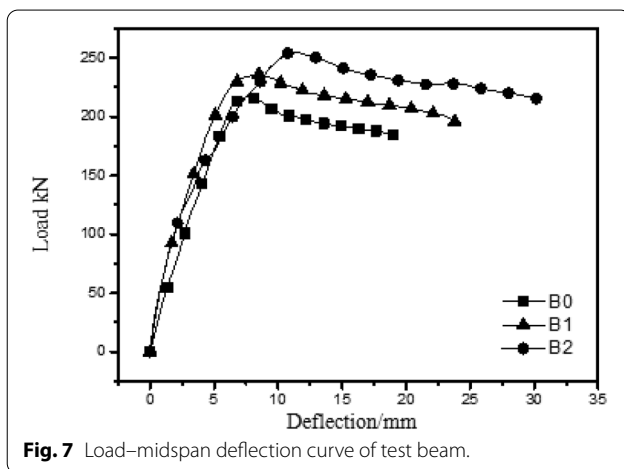


Fig. 7 Load–midspan deflection curve of test beam.

(3) Load–deflection curves were analyzed. The curve began to descend immediately after the conventional reinforced-concrete beam B0 reached the ultimate bearing capacity, and the bearing capacity fell rapidly when the deflection did not increase obviously. The curve in Fig. 7 is steeper and the initial descending slope is larger than the curves of beams that were mixed with polypropylene fiber and multisize polypropylene fiber concrete beams, which showed a less sudden drop after reaching the limit load value. The bearing capacity decreased along a relatively smooth curve. The load–deflection curve of the multisize polypropylene fiber concrete beam B2 was most saturated, which shows that the multisize polypropylene fiber can improve the ultimate bending load-bearing capacity of the concrete beam, and increase the ductility of the beam and provide a significant crack resistance and toughening effect.

3.2 Comparison of Cracking Loads

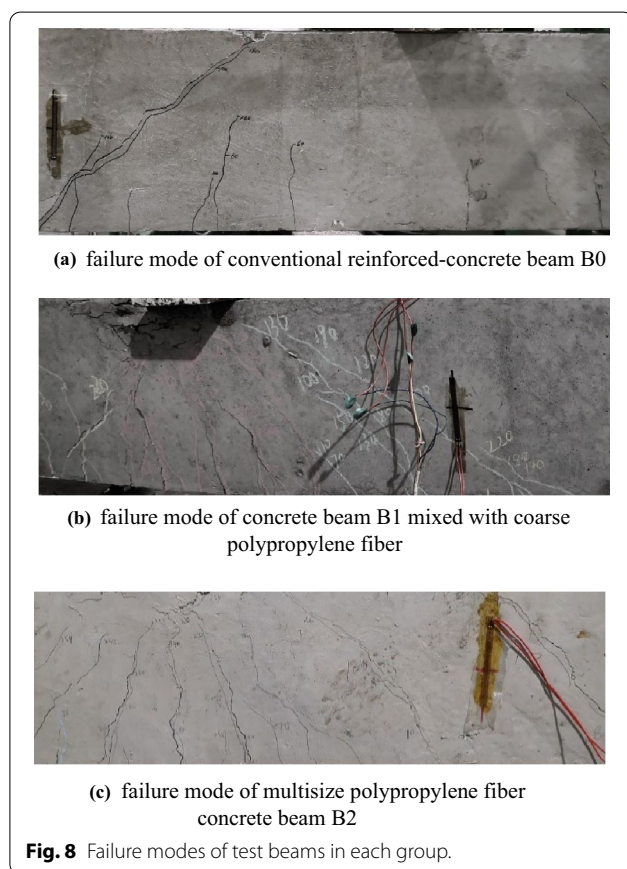
During loading, crack occurrence in the test beams was observed, and the cracking load data were collected immediately when cracks were observed. A ZBL-F130 crack width observation instrument was used to measure the crack width. The cracking loads of the three groups of shear test beams and their corresponding crack widths are shown in Table 5.

By analyzing the cracking load and crack width of test beams, the following results were obtained:

- (1) By taking the average value of the cracking load of each group of concrete beams with different fiber-reinforcement dosages, it can be concluded that the cracking load of conventional reinforced-concrete beams is 57.45 kN, the cracking load of concrete beams mixed with coarse polypropylene fibers only is 76.97 kN, and the cracking load of concrete beams mixed with three fiber types is 92.21 kN. Compared with conventional reinforced-concrete beams, the cracking load of concrete mixed with coarse polypropylene fibers only increased by 33.98%, and that of multisize polypropylene fiber concrete beams increased by 60.50%.
- (2) Compared the initial crack widths of the three specimens, the initial crack width of conventional reinforced-concrete beams without fiber is largest, and the initial crack widths of B1 and B2 mixed with fibers were reduced. According to the test results, the initial crack of the multisize polypropylene fiber concrete beams was smallest, which shows that polypropylene fibers of different sizes play a supporting and complementary role, form a spatial network structure, enhance the beam toughness and inhibit crack development.

Table 5 Cracking load and crack width of test beam.

Test beam no.	Cracking load (kN)	Average cracking load (kN)	Standard deviation of the average load (kN)	Crack width (mm)	Average crack width (mm)	Standard deviation of the average crack width (mm)
B0	B0-1	60.23	57.45	2.03	0.060	0.000943
	B0-2	55.42			0.062	
	B0-3	56.71			0.060	
B1	B1-1	75.13	76.97	1.33	0.043	0.00330
	B1-2	78.21			0.038	
	B1-3	77.58			0.035	
B2	B2-1	90.43	92.21	1.43	0.043	0.00942
	B2-2	93.94			0.026	
	B2-3	92.25			0.021	



3.3 Crack Shape and Failure Mode

The failure mode and crack shape of the test beams are shown in Fig. 8a, b and c, in which Fig. 8a is the failure mode of conventional reinforced-concrete beam B0, Fig. 8b is the failure mode of concrete beam B1 mixed with coarse polypropylene fiber, and Fig. 8c is the failure mode of multisize polypropylene fiber concrete beam B2. According to the crack development and failure of test beams, the following can be seen:

As shown on the left of Fig. 8a, initially, concrete beam B0 without polypropylene fiber shows vertical cracks at the bending and shearing sections of the beam, and when the load increases, the amount of vertical bending cracks increase, but the development is slow, and the width is relatively balanced. When the load increases continuously, a bending and shearing section were observed, a number of small oblique cracks existed and developed gradually into main oblique cracks, as shown on the right of Fig. 8a. Along with the rapid development of main crack width and continuous local compression crushing, the main crack grew, coalesced gradually, and finally lead to failure. During this process, vertical bending cracks were observed, and their number increased continuously in the early stage, but did not increase obviously in the later stage. The width and height of the main oblique cracks were large, which resulted in shear failure.

As shown on the left of Fig. 8b, crack development of concrete beam B1 mixed with coarse polypropylene fibers is basically the same as that of the conventional reinforced-concrete beam in the initial stage. However, when failure occurs, although a large main oblique crack existed, it did not develop into a critical oblique crack that leads to beam failure. Instead, concrete in the compression zone was crushed after the tensile reinforcement near the support yielded, which resulted in flexural-shear failure. The right figure of Fig. 8b shows that coarse fiber mixed into the concrete beam plays a good bridging role. When the specimen was stressed, the fiber could absorb some energy and hinder crack extension.

As shown on the left of Fig. 8c, multisize polypropylene fiber concrete beam B2 was mixed with one type of coarse polypropylene fiber and two types of fine polypropylene fibers that were crushed in the compression zone after the tensile reinforcement at the support yielded, which resulted in bending-shear failure with obvious plastic characteristics. Compared with polypropylene fiber concrete beams that were mixed with coarse fibers

only (B1), the cracks were more densely distributed, and the beams had a larger deflection, better ductility and greater ultimate bearing capacity. The crack shape on the right of Fig. 8c showed that because the difference between the diameter of polypropylene fine fiber and the width of microcrack is very close, which can ensure a sufficient cohesive length with concrete, fine fibers can prevent continuous expansion at the microcrack expansion stage. However, when the microcrack width developed to a certain extent, the bearing capacity and bonding force of a single fine fiber were small, and the fiber was disconnected or pulled out, the connection effect was lost, and the development of wider cracks was no longer inhibited. As the number of cracks continued to increase, coarse fibers began to inhibit macrocracks and hinder the development of wider cracks until they were pulled out.

A comparison between concrete beam B0 without polypropylene fibers and concrete beam B1 with coarse polypropylene fibers, shows that polypropylene fiber addition increases the deformation capacity, changes the brittle shear failure to a plastic bending-shear failure, which changes the beam failure mode. The addition of coarse polypropylene fibers improves the beam plasticity, which increases the beam toughness.

A comparison between multisize polypropylene fiber concrete beams B2 with concrete beams B1 mixed with coarse polypropylene fibers only, shows that B2 beam has a higher load-bearing capacity, a greater plasticity, produces more and denser cracks, but a narrower width. The concrete performance improved after mixed multisize polypropylene fibers were added. The three fibers can interact to make up for the deficiency of the single fiber, support each other, form a whole and build a spatial network structure in the concrete, which will increase the concrete performance and beam toughness, and improve the ductility.

3.4 Analysis of Concrete Beam Deformation

To study the influence of polypropylene fibers on the concrete deformation of the test beams, an analysis and study of strains of conventional reinforced-concrete beam B0 without polypropylene fiber, concrete beam B1 with coarse polypropylene fibers and multisize polypropylene fiber concrete beam B2 was carried out. In tests of three groups, the through the thickness strain of concrete in a section near the middle of the span was compared and analyzed.

The through the thickness strain curves of concrete for B0, B1 and B2 beams under different loads are shown in Fig. 9.

An analysis of the three strain curves showed that at the initial stage of loading, for the through the thickness strain, the following relationship was obtained:

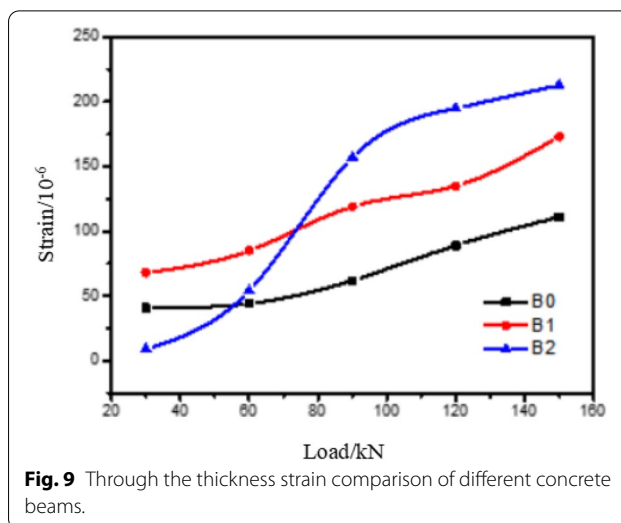


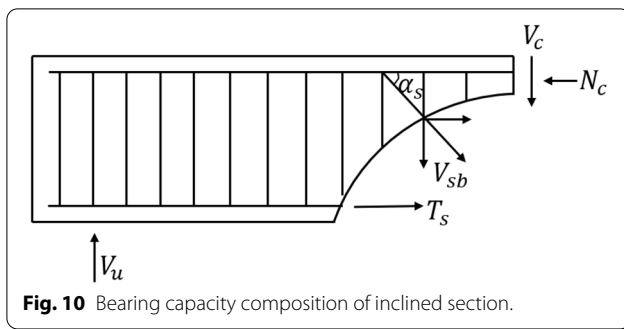
Fig. 9 Through the thickness strain comparison of different concrete beams.

conventional reinforced-concrete beam through the thickness strain is larger than that of multisize polypropylene fiber concrete beam, and is smaller than that of concrete beams mixed with coarse fibers. Coarse fiber addition increases the initial defects of the concrete structure and increases the strain, but the fine fiber in the multisize polypropylene fiber can improve the performance in the initial loading stage. Thus, the concrete can bear more force in a smaller deformation state. The curves of B0 and B1 are basically the same in the middle and later stages of loading analysis, but the multisize polypropylene fiber concrete has a greater strain in the transverse direction. These results show that multisize polypropylene fibers can enhance the plastic deformation capacity of concrete, improve the brittle failure of the beam, and enhance the ultimate shear-bearing capacity of the concrete beam.

4 Study on Modification of Calculation Formula for Shear Capacity of Polypropylene Fiber Concrete Beams

According to the calculation formula in the *Technical Specification for Design of Concrete Structures* (GB50010-2010) (GB, 2010) and based on the characteristics of polypropylene fibers, the formula was modified to obtain a formula to calculate the shear-bearing capacity of polypropylene fiber concrete beams. The theoretical calculation in this paper includes the following main assumptions:

- (1) When the beam was subjected to shear and compression failure, and with a consideration for the force balance condition, as shown in Fig. 10, the design



value of the inclined section shear force of the beam consisted of the following three parts:

$$V_u = V_c + V_s + V_{sb}, \tag{1}$$

where V_u is the design value of the ultimate shear-bearing capacity of concrete beams, V_c is the design value of the shear-bearing capacity of the concrete shear compression zone, V_s is the design value of the shear-bearing capacity of the stirrup that intersects the inclined cracks and V_{sb} is the design value of the shear-bearing capacity of the bending reinforcement with inclined cracks.

Because V_c and V_s are related closely in the actual calculation and cannot be calculated separately, V_{cs} is used to represent the resultant shear capacity of the concrete and stirrups. Because test beams were not equipped with an inclined reinforcement, there was no need to consider V_{sb} , namely:

$$V_u = V_{cs} = V_c + V_s. \tag{2}$$

- (2) When the beam reached the limit of shear-compression failure, the stirrups that intersected the inclined cracks yielded.
- (3) For beams with a web reinforcement, the influence of section size was not considered.
- (4) For concrete beams with no inclined reinforcement and only stirrups under concentrated loads, the following calculation formula was given in the *Technical Specification for Design of Concrete Structures* (GB50010-2010) (GB, 2010):

$$V_u = V_{cs} = \frac{1.75}{\lambda + 1} f_t b h_0 + f_{yv} \frac{A_{sv}}{s} h_0, \tag{3}$$

where f_t is the concrete tensile strength, f_{yv} is the design value of the stirrup tensile strength, b is the cross-sectional width of the concrete beam, h_0 is the effective

Table 6 Fiber characteristic parameter and fiber-reinforcement coefficient of test beams.

Test beam no.	Fiber characteristic parameter λ_f	Fiber reinforcement coefficient β_v
B0	0	0
B1	0.39	0.151
B2	0.91	0.156

cross-sectional height of the concrete beam, and λ is used to calculate the shear span ratio of the cross-section. When $\lambda < 1.5$, $\lambda = 1.5$ and when $\lambda > 3$, $\lambda = 3$. s is the stirrup spacing along the length direction of the member, and A_{sv} is the cross-sectional area of the stirrup in the same cross-section.

For polypropylene fiber concrete beams, fiber addition changes the cohesiveness between the reinforcement and the concrete and increases the bonding stress, according to reference (Zhao et al., 1999). Cracks will appear in the concrete under the action of an external force. The position of the surrounding reinforcement and concrete will change, which leads to bond slip. However, this situation will be delayed after fiber addition. Therefore, the bonding stress is considered to relate to the fiber length l_f , diameter d_f and fiber volume fraction ρ_f . Among them, the fiber characteristic parameter λ_f is the product of the fiber volume fraction and the length-to-diameter ratio l_f/d_f .

Based on the test results and theoretical analysis, reference Zhao et al., (1999) modifies the formula of the shear-bearing capacity of the inclined section of the concrete beam with a fiber-reinforcement coefficient β_v and a characteristic fiber parameter λ_f , and proposes the formula for shear-bearing capacity V_{fu} of the fiber concrete beam under concentrated loads:

$$V_{fu} = V_{cs} = \frac{1.75}{\lambda + 1} (1 + \beta_v \lambda_f) f_t b h_0 + f_{yv} \frac{A_{sv}}{s} h_0. \tag{4}$$

According to the data under inclined section shear failure and the fiber characteristic parameter λ_f of the inclined section shear test beam, the fiber-reinforcement coefficient β_v was calculated, and results are shown in Table 6.

According to Eq. (4), the ultimate bending bearing capacity of the inclined sections of the three groups of test beams in this paper was calculated, and an analysis and comparison between the test values and theoretical calculation values were carried out. The results are shown in Table 7.

According to the calculation results, the ratio of measured to theoretical value that was calculated by the

Table 7 Comparison between calculated and measured shear capacity of beam sections.

Test beam no.	Measured value (kN)	Average measured value (kN)	Standard deviation of the average measured value (kN)	Calculated value (kN)	Measured value/calculated value
B0-1	108.55	109.40	0.62	102.01	1.064
B0-2	110.00			102.01	1.078
B0-3	109.64			102.01	1.075
B1-1	114.83	118.23	3.28	114.39	1.004
B1-2	122.66			114.39	1.072
B1-3	117.19			114.39	1.024
B2-1	131.97	128.52	2.52	130.96	1.008
B2-2	126.04			130.96	0.962
B2-3	127.55			130.96	0.974

modified formula of the ultimate shear-bearing capacity of the inclined section of the test beams was 1.029 on average, with a standard deviation of 0.04, and a variable coefficient of 0.04. The calculated value was consistent with the measured value.

5 Conclusions

By carrying out three groups of inclined section shear tests of reinforced concrete rectangular beams with different fiber contents, the shear performance of multisize polypropylene fiber concrete beams was determined in terms of load–midspan deflection, cracking load comparison, crack shape and failure mode, and concrete deformation. Through in-depth analysis, the following recommendations were reached:

- (1) Polypropylene fiber addition can improve the shear-bearing capacity of rectangular beams. Compared with conventional reinforced-concrete beam B0 (fiber content: none), the limit shear load of concrete beam B1 mixed with coarse polypropylene fibers (fiber content: CF1, 6 kg/m³) and multisize polypropylene fiber concrete beam B2 mixed with three kinds of fibers (fiber content: FF1, 0.6 kg/m³; FF2, 0.6 kg/m³; CF1, 4.8 kg/m³) increased by 8.67% and 17.07%, respectively.
- (2) Polypropylene fiber addition into concrete beams can improve the initial crack shear force of beams, inhibit crack development, increase the number of cracks and reduce the crack width, which can increase the beam ductility and achieve crack resistance and toughening. For the same total fiber content, the crack resistance and toughening effect of beams with multisize polypropylene fibers B2 is better than that with coarse polypropylene fibers B1. When the dosage was the same, the multisize polypropylene fiber B2 could improve the shear capacity of the inclined section of the beam most.

- (3) Based on Code for Design of Concrete Structures (GB50010-2010), the theoretical calculation of the ultimate bearing capacity of the test beams was carried out and improved, and the calculation results were consistent with the test values.

Acknowledgements

Not applicable.

Authors' contributions

NL analyzed the experiments, XY and RF wrote the manuscript, YH conducted the experiments. All authors read and approved the final manuscript.

Authors' information

Xin Yang, Associate Professor, School of Civil Engineering, Chongqing University, Chongqing 400045, China. Ninghui Liang, Associate Professor, School of Civil Engineering, Chongqing University, Chongqing 400045, China. Yang Hu, Postgraduate Student, School of Civil Engineering, Chongqing University, Chongqing 400045, China. Rui Feng, Master, Henan Metallurgical Planning and Design Research Institute Co. LTD, Zhengzhou 450000, China.

Funding

This study is supported by Training Plan for Outstanding Young Scientific Research Talents in Colleges and Universities of Fujian Province (Grant No. GY-Z18160), the National Natural Science Foundation of China (Grant No. 41372356), we gratefully acknowledge these supports.

Availability of data and materials

The datasets used and/or analyzed during the current study are available from the corresponding author on reasonable request.

Declarations

Competing interests

The authors declare that they have no known competing financial interests or personal relationships that could have appeared to influence the work reported in this paper.

Author details

¹School of Civil Engineering, Chongqing University, Chongqing 400045, China. ²Key Laboratory of New Technology for Construction of Cities in Mountain Area (Chongqing University), Ministry of Education, Chongqing 400030, China. ³School of Civil Engineering, Fujian University of Technology, Fuzhou 350108, China. ⁴Henan Metallurgical Planning and Design Research Institute Co. LTD, Zhengzhou 450000, China.

Received: 5 May 2021 Accepted: 9 December 2021
Published online: 24 December 2021

References

- Abdelrazik, A. T., & Khayat, K. H. (2020). Effect of fiber characteristics on fresh properties of fiber reinforced concrete with adapted rheology. *Construction and Building Materials*, 230, UNSP 116852.
- Aoude, H., Belghiti, M., Cook, W. D., & Mitchell, D. (2012). Response of steel fiber-reinforced concrete beams with and without stirrups. *ACI Structural Journal*, 109(3), 359–367.
- Arslan, G., Keskin, R. S. O., & Ozturk, M. (2017). Shear behaviour of polypropylene fibre-reinforced-concrete beams without stirrups. *Proceedings of the Institution of Civil Engineers: Structures and Buildings*, 170(3), 190–198.
- Asgari, M. A., Mastali, M., Dalvand, A., & Abdollahnejad, Z. (2019). Development of deflection hardening cementitious composites using glass fibres for flexural repairing/strengthening concrete beams: Experimental and numerical studies. *European Journal of Environmental and Civil Engineering*, 23(8), 916–944.
- Cardoso, D. C. T., Pereira, G. B. S., Silva, F. A., Silva, J. J. H., & Pereira, E. V. (2019). Influence of steel fibers on the flexural behavior of RC beams with low reinforcing ratios: Analytical and experimental investigation. *Composite Structures*, 222, UNSP 110926.
- Das, C. S., Dey, T., Dandapat, R., Mukharjee, B. B., & Kumar, J. (2018). Performance evaluation of polypropylene fibre reinforced recycled aggregate concrete. *Construction and Building Materials*, 189, 649–659.
- Deng, F. Q., Ding, X. X., Chi, Y., & Xu, L. H. (2018). The pull-out behavior of straight and hooked-end steel fiber from hybrid fiber reinforced cementitious composite: Experimental study and analytical modelling. *Composite Structures*, 206, 693–712.
- Ferreira, L. E. T., de Hanai, J. B., & Ferrari, V. J. (2016). Optimization of a hybrid-fiber-reinforced high-strength concrete. *Mechanics of Composite Materials*, 52(3), 295–304.
- Gail, S., & Subramaniam, K. V. (2019). Cohesive stress transfer and shear capacity enhancements in hybrid steel and macro-polypropylene fiber reinforced concrete. *Theoretical and Applied Fracture Mechanics*, 103, 102250.
- GB 50010-2010. (2010). Technical specification for design of concrete structure. China Architecture & Building Press.
- Hameed, R., Hasnain, K., Riaz, M. R., Khan, Q. S., & Siddiqi, Z. A. (2020). Reinforced fibrous recycled aggregate concrete element subjected to uniaxial tensile loading. *Advances in Concrete Construction*, 9(2), 195–205.
- Hu, H. T., Lin, F. M., & Jan, Y. Y. (2004). Nonlinear finite element analysis of reinforced concrete beams strengthened by fiber-reinforced plastics. *Composite Structures*, 63(3–4), 271–281.
- Huang, L., Xu, L. H., Chi, Y., Deng, F. Q., & Zhang, A. L. (2019). Bond strength of deformed bar embedded in steel-polypropylene hybrid fiber reinforced concrete. *Construction and Building Materials*, 218, 176–192.
- JGJ 55-2019. (2019). Technical specification for mix proportion design of conventional concrete. China Architecture & Building Press.
- Khalid, F. S., Irwan, J. M., Ibrahim, M. H. W., Othman, N., & Shahidan, S. (2018). Performance of plastic wastes in fiber-reinforced concrete beams. *Construction and Building Materials*, 183, 451–464.
- Khan, A. R., Al-Gadhib, A. H., & Baluch, M. H. (2011). Experimental and computational modeling of low cycle fatigue damage of CFRP strengthened reinforced concrete beams. *International Journal of Damage Mechanics*, 20(2), 211–243.
- Koniki, S., & Prasad, D. R. (2019). Influence of hybrid fibres on strength and stress-strain behaviour of concrete under uni-axial stresses. *Construction and Building Materials*, 207, 238–248.
- Lee, J. H. (2017). Influence of concrete strength combined with fiber content in the residual flexural strengths of fiber reinforced concrete. *Composite Structures*, 168, 216–225.
- Liu, J. Z., Han, F. Y., Cui, G., Zhang, Q. Q., Lv, J., Zhang, L. H., & Yang, Z. Q. (2016). Combined effect of coarse aggregate and fiber on tensile behavior of ultra-high performance. *Construction and Building Materials*, 121, 310–318.
- Ma, K. Z., Qi, T., Liu, H. J., & Wang, H. B. (2018). Shear behavior of hybrid fiber reinforced concrete deep beams. *Materials*, 11(10), 2023.
- Meesala, C. R. (2019). Influence of different types of fiber on the properties of recycled aggregate concrete. *Structural Concrete*, 20(5), 1656–1669.
- Melian, G., Barluenga, G., & Hernandez-Olivares, F. (2010). Toughness increase of self-compacting concrete reinforced with polypropylene short fibers. *Materiales De Construccion*, 60(300), 83–97.
- Navas, F. O., Navarro-Gregori, J., Leiva, G., & Serna, P. (2020). Comparison of macrosynthetic and steel FRC shear-critical beams with similar residual flexure tensile strengths. *Structural Engineering and Mechanics*, 76(4), 491–503.
- Nordin, H., & Taljsten, B. (2004). Testing of hybrid FRP composite beams in bending. *Composites Part b: Engineering*, 35(1), 27–33.
- Raja, R. B., & Sivakumar, M. V. N. (2020). Influence of coarse aggregate properties on specific fracture energy of steel fiber reinforced self compacting concrete. *Advances in Concrete Construction*, 9(2), 173–181.
- Sahoo, D. R., Solanki, A., & Kumar, A. (2015). Influence of steel and polypropylene fibers on flexural behavior of RC beams. *Journal of Materials in Civil Engineering*, 27(8), 04014232.
- Saje, D., Bandelj, B., Sustersic, J., Lopatic, J., & Saje, F. (2011). Shrinkage of polypropylene fiber-reinforced high performance concrete. *Journal of Materials in Civil Engineering*, 23(7), 941–952.
- Spinella, N., Colajanni, P., & La Mendola, L. (2012). Nonlinear analysis of beams reinforced in shear with stirrups and steel fibers. *ACI Structural Journal*, 109(1), 53–63.
- Thomas, J., & Ramaswamy, A. (2006). Shear strength of prestressed concrete T-beams with steel fibers over partial/full depth. *ACI Structural Journal*, 103(3), 427–435.
- Xu, L. H., Deng, F. Q., & Chi, Y. (2017). Nano-mechanical behavior of the interfacial transition zone between steel-polypropylene fiber and cement paste. *Construction and Building Materials*, 145, 619–638.
- Younis, A., Ebead, U., Suraneni, P., & Nanni, A. (2020). Short-term flexural performance of seawater-mixed recycled-aggregate GFRP-reinforced concrete beams. *Composite Structures*, 236, UNSP 111860.
- Zhang, L. H., Liu, J. Z., Liu, J. P., Zhang, Q. Q., & Han, F. Y. (2018). Effect of steel fiber on flexural toughness and fracture mechanics behavior of ultrahigh performance concrete with coarse aggregate. *Journal of Materials in Civil Engineering*, 30(12), 04018323.
- Zhang, R., Matsumoto, K., Hirata, T., Ishizeki, Y., & Niwa, J. (2014). Shear behavior of polypropylene fiber reinforced ECC beams with varying shear reinforcement ratios. *Journal of JSCE*, 2(1), 39–53.
- Zhao, G. F., Peng, S. M., & Huang, C. K. (1999). *Steel fiber reinforced concrete structure*. China Architecture & Building Press.

Publisher's Note

Springer Nature remains neutral with regard to jurisdictional claims in published maps and institutional affiliations.

Submit your manuscript to a SpringerOpen[®] journal and benefit from:

- Convenient online submission
- Rigorous peer review
- Open access: articles freely available online
- High visibility within the field
- Retaining the copyright to your article

Submit your next manuscript at ► [springeropen.com](https://www.springeropen.com)